

## Supporting information

Suwiat Sangon<sup>a</sup>, Kanokwan Kotebantao<sup>a</sup>, Theerakan Suyala<sup>a</sup>, Yuvarat Ngernyen<sup>b</sup>, Andrew J. Hunt<sup>a</sup> and Nontipa Supanchaiyamat<sup>a\*</sup>

<sup>a</sup> Material Chemistry Research center, Department of Chemistry, and center of excellent for innovation in Chemistry, Faculty of Science, Khon Kaen University, Khon Kaen, 40002, Thailand

<sup>b</sup> Department of Chemical Engineering, Faculty of Engineering, Khon Kaen University, Khon Kaen, 40002, Thailand

The UV-Vis absorption spectra of amoxicillin at different concentrations demonstrates a maximum wavelength at 195 nm as presented in the figure S1 below. This wavelength was selected for analysis of all samples containing amoxicillin.

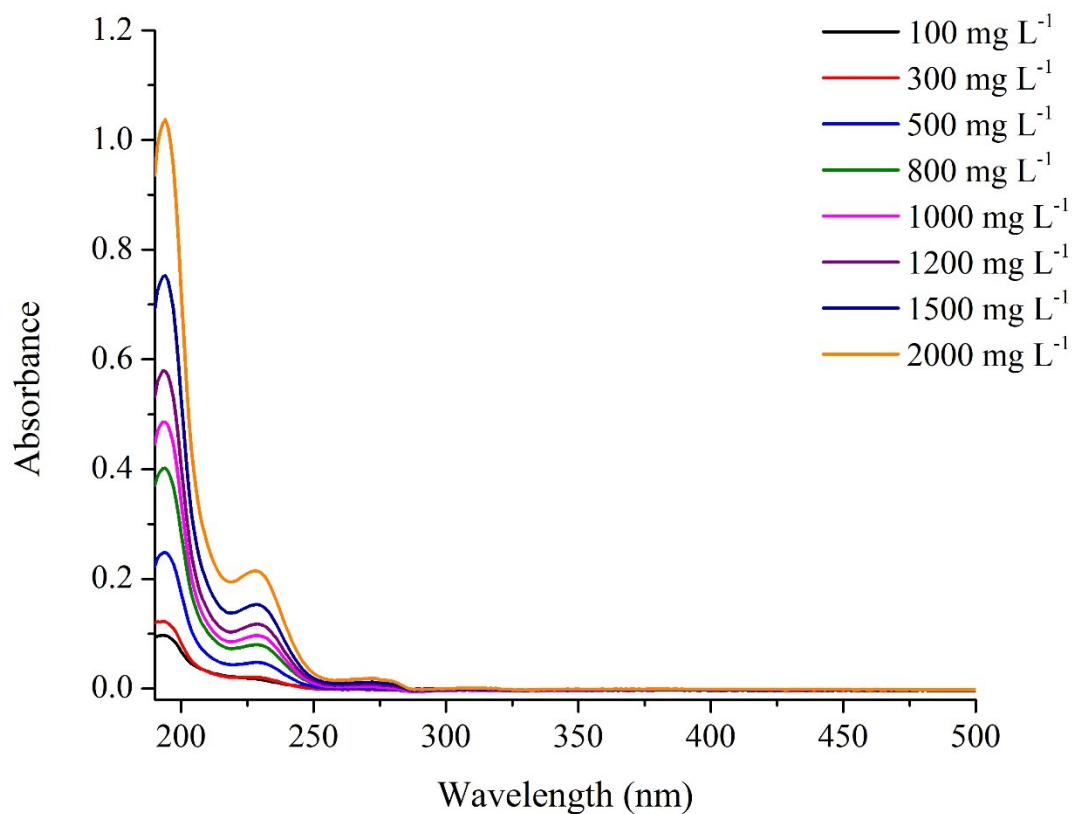


**Figure S1** UV-Vis absorption spectra of amoxicillin

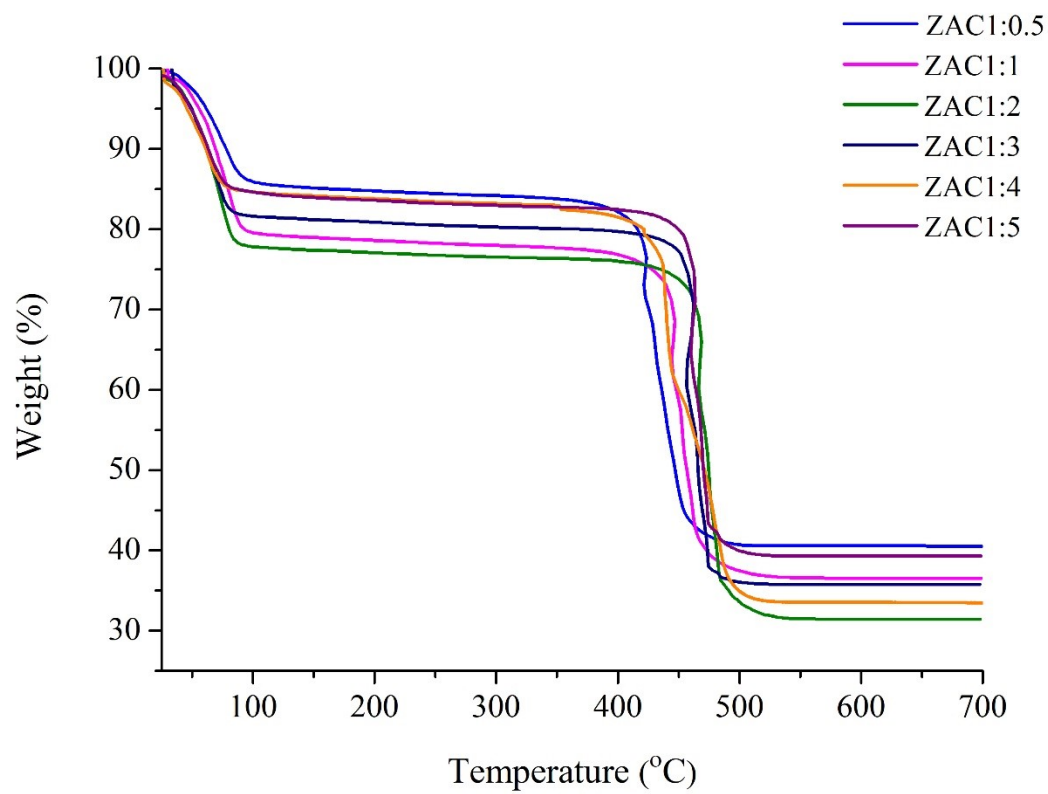


**Figure S2** TGA thermograms of ZnCl<sub>2</sub>-activated carbon

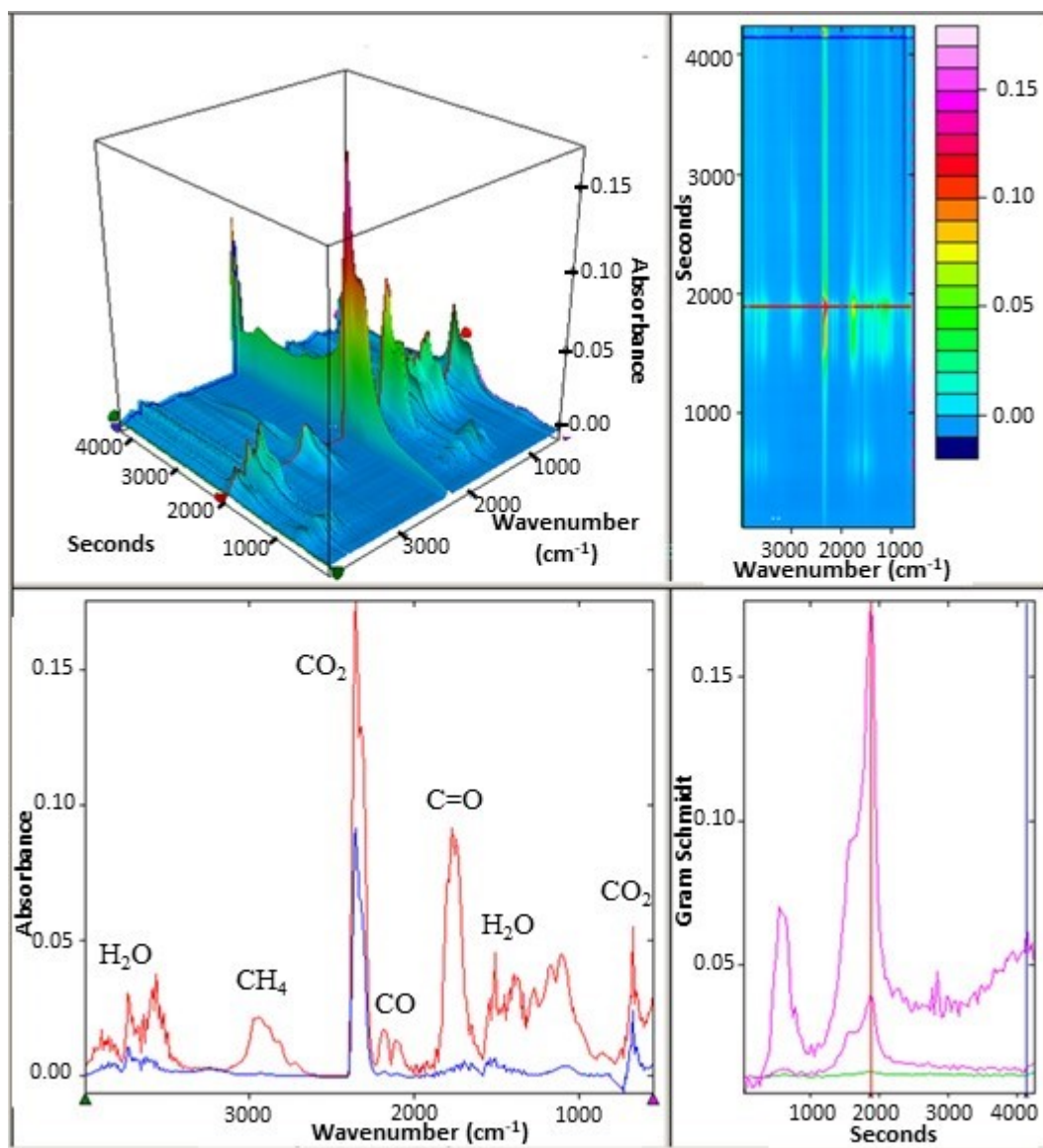


**Figure S3** TGA-IR analysis of rice straw during pyrolysis (top-left image: 3D plot of TGA-IR time-series, top-right image: color indication of IR spectra intensity, bottom-left image: IR spectra at 340 °C (red) and 700 °C (blue), bottom-right image: Gram-Schmidt graph).

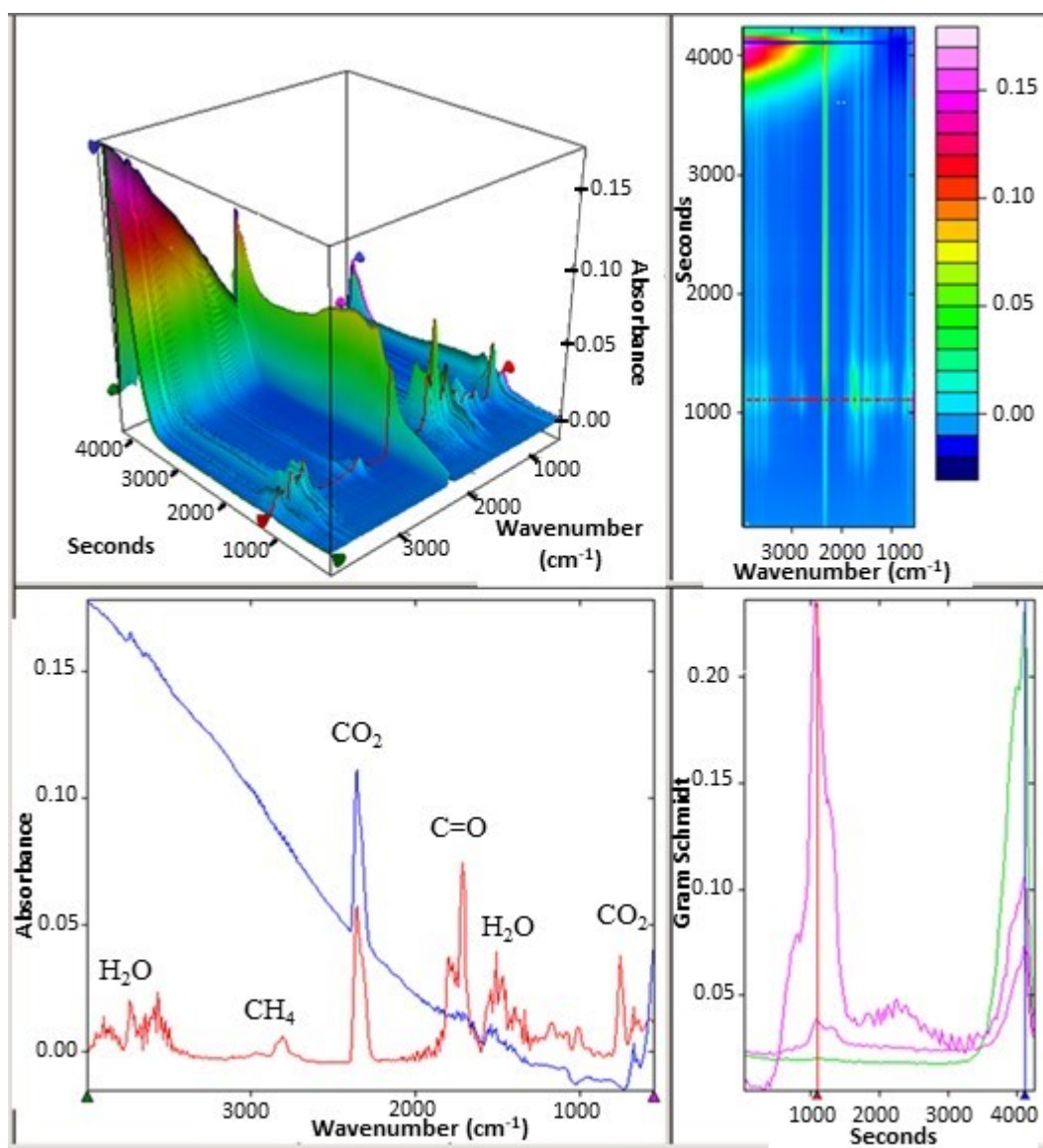


**Figure S4** TGA-IR analysis of ZAC1:0.5 during pyrolysis (top-left image: 3D plot of TGA-IR time-series, top-right image: color indication of IR spectra intensity, bottom-left image: IR spectra at 195 °C (red) and 700 °C (blue), bottom-right image: Gram-Schmidt graph).

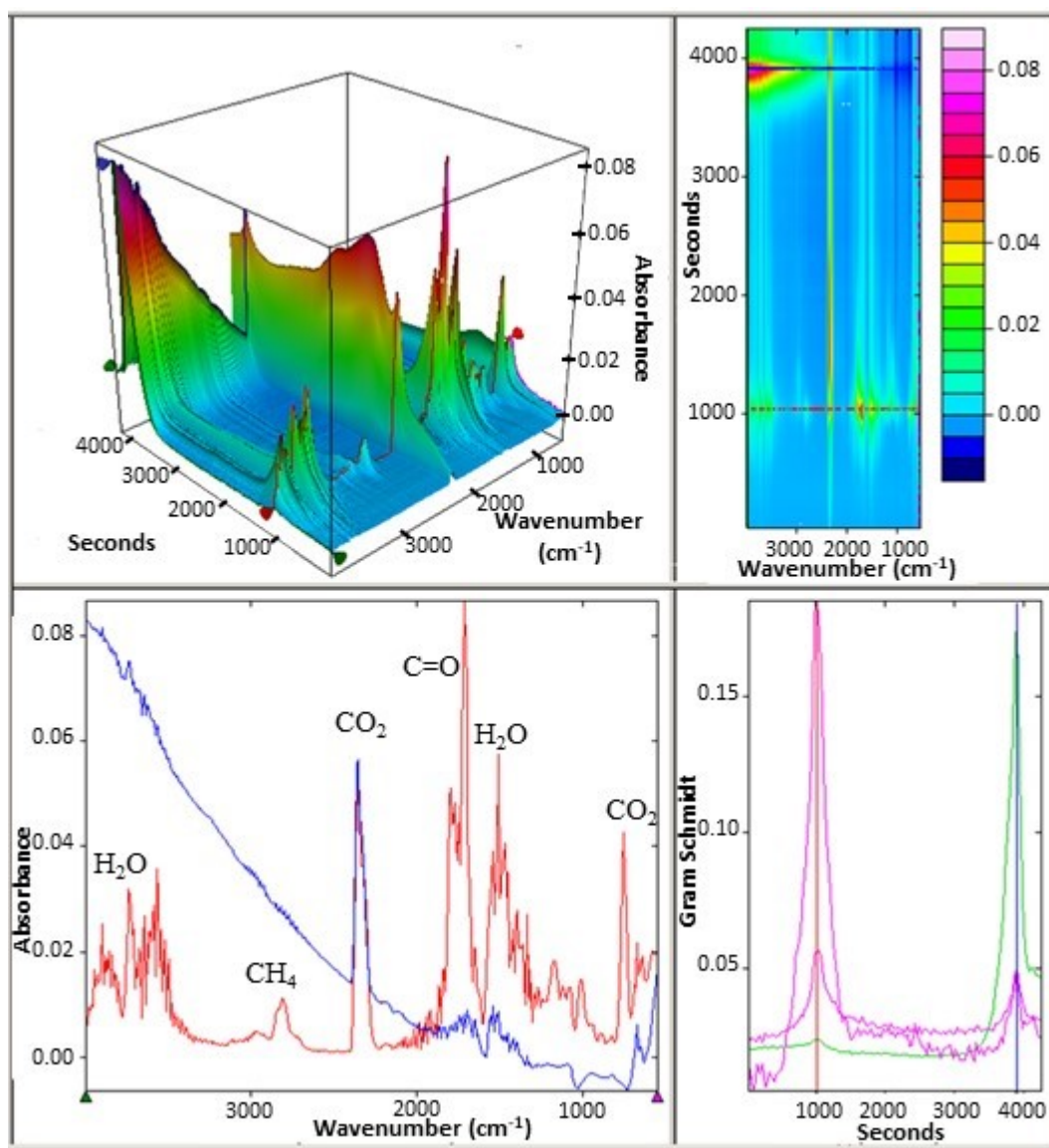


**Figure S5** TGA-IR analysis of ZAC1:1 during pyrolysis (top-left image: 3D plot of TGA-IR time-series, top-right image: color indication of IR spectra intensity, bottom-left image: IR spectra at 195 °C (red) and 700 °C (blue), bottom-right image: Gram-Schmidt graph).

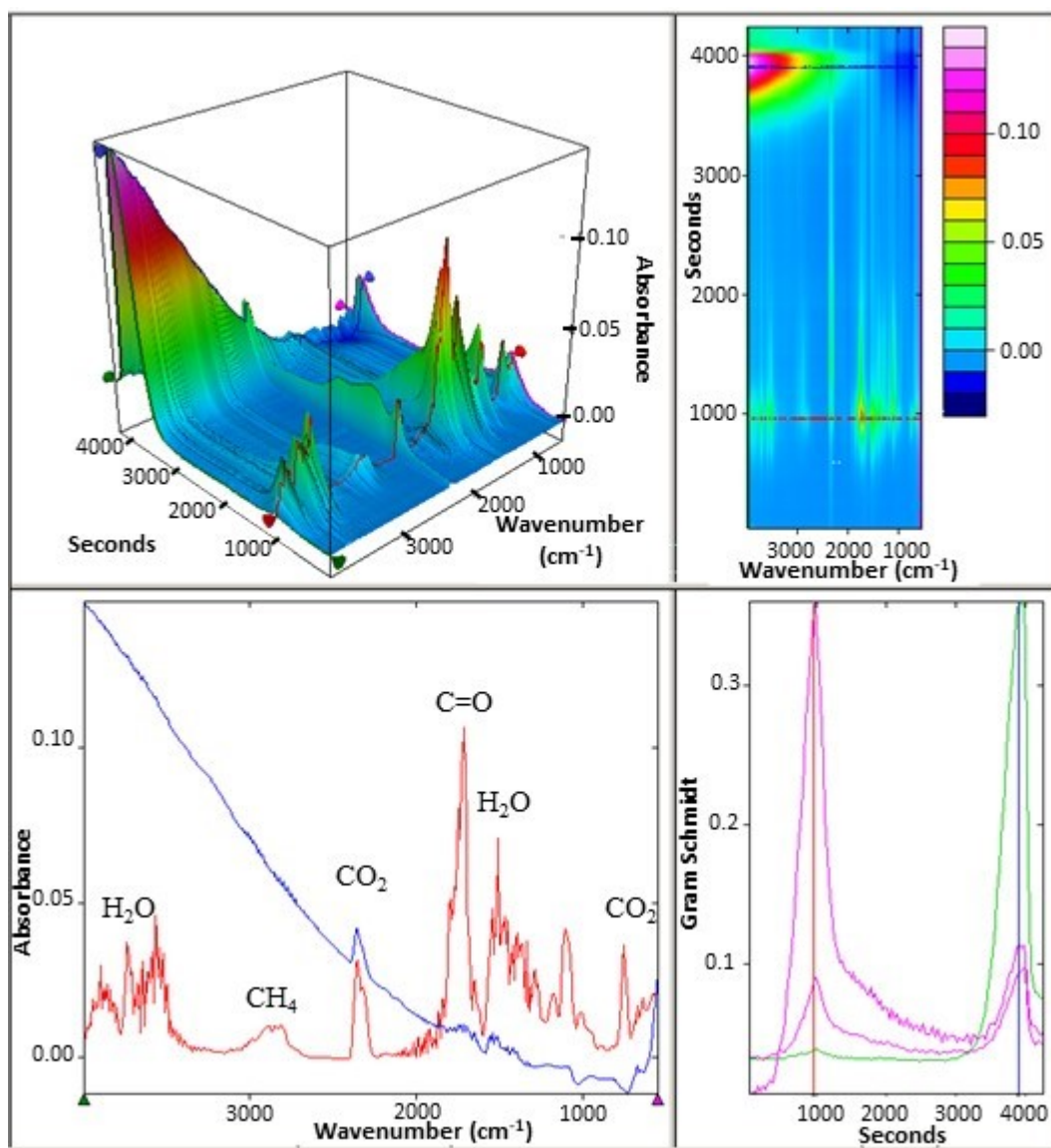


**Figure S6** TGA-IR analysis of ZAC1:2 during pyrolysis (top-left image: 3D plot of TGA-IR time-series, top-right image: color indication of IR spectra intensity, bottom-left image: IR spectra at 195 °C (red) and 700 °C (blue), bottom-right image: Gram-Schmidt graph).

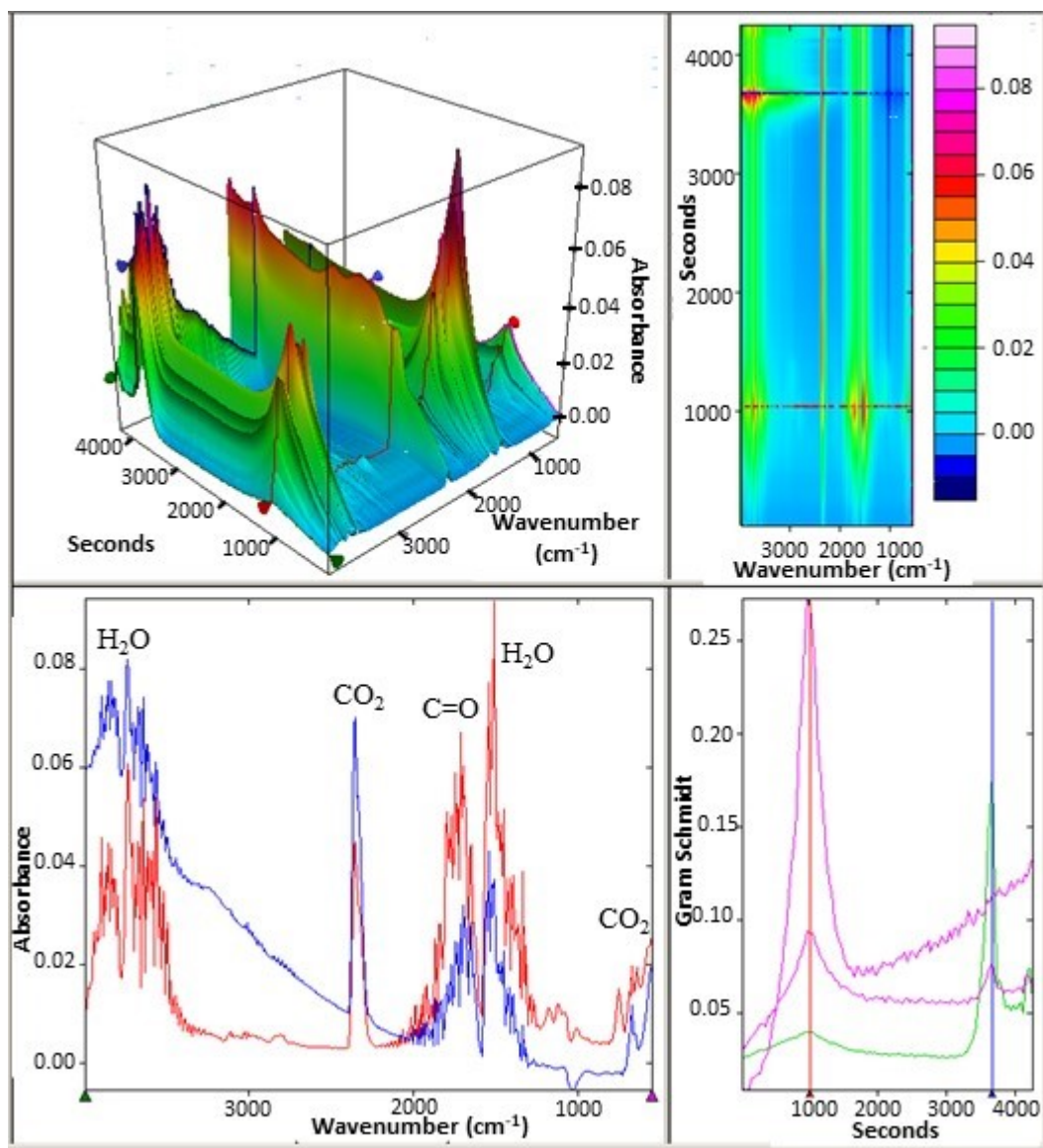


**Figure S7** TGA-IR analysis of ZAC1:3 during pyrolysis (top-left image: 3D plot of TGA-IR time-series, top-right image: color indication of IR spectra intensity, bottom-left image: IR spectra at 195 °C (red) and 700 °C (blue), bottom-right image: Gram-Schmidt graph).

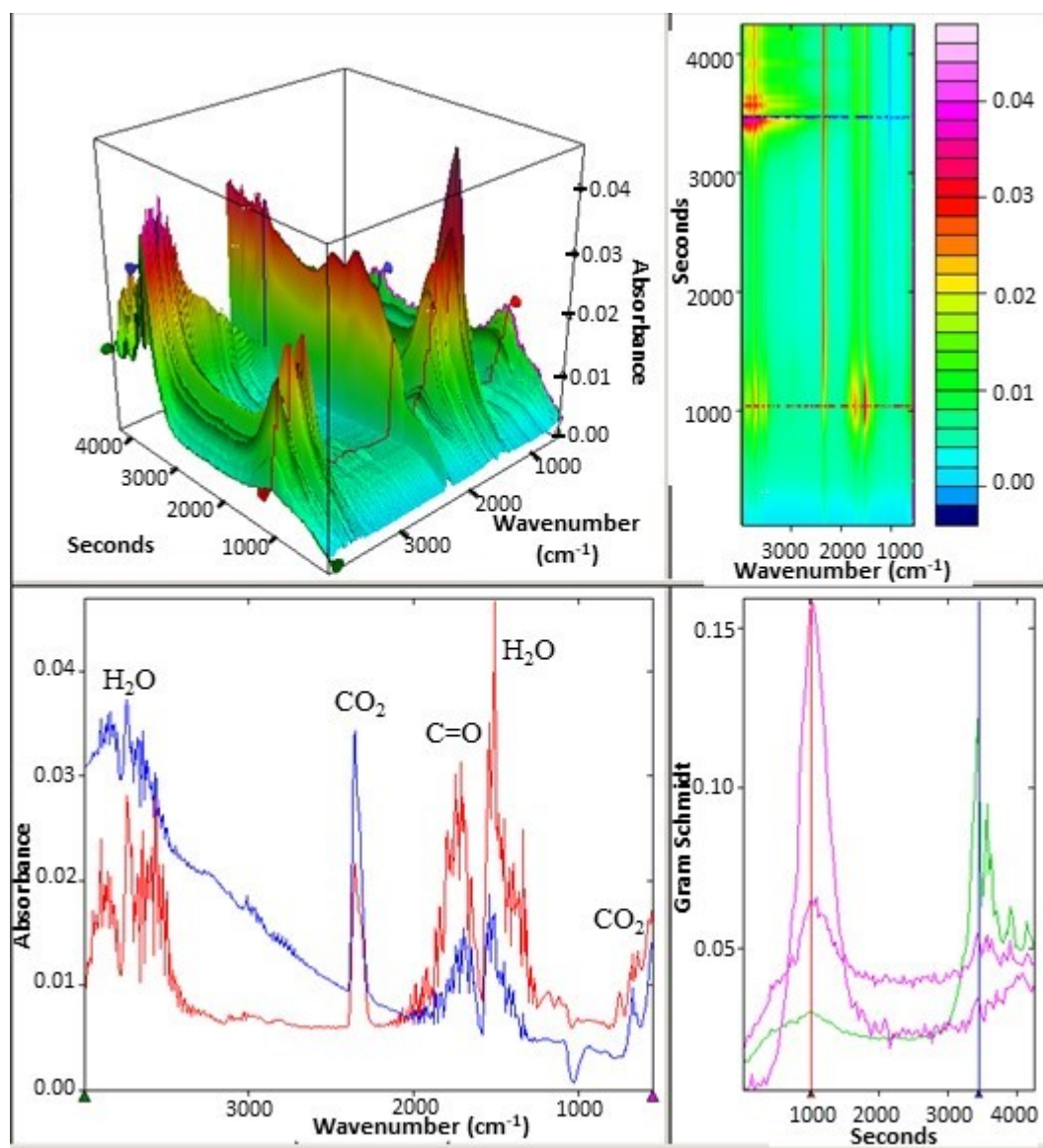


**Figure S8** TGA-IR analysis of ZAC1:4 during pyrolysis (top-left image: 3D plot of TGA-IR time-series, top-right image: color indication of IR spectra intensity, bottom-left image: IR spectra at 195 °C (red) and 700 °C (blue), bottom-right image: Gram-Schmidt graph).

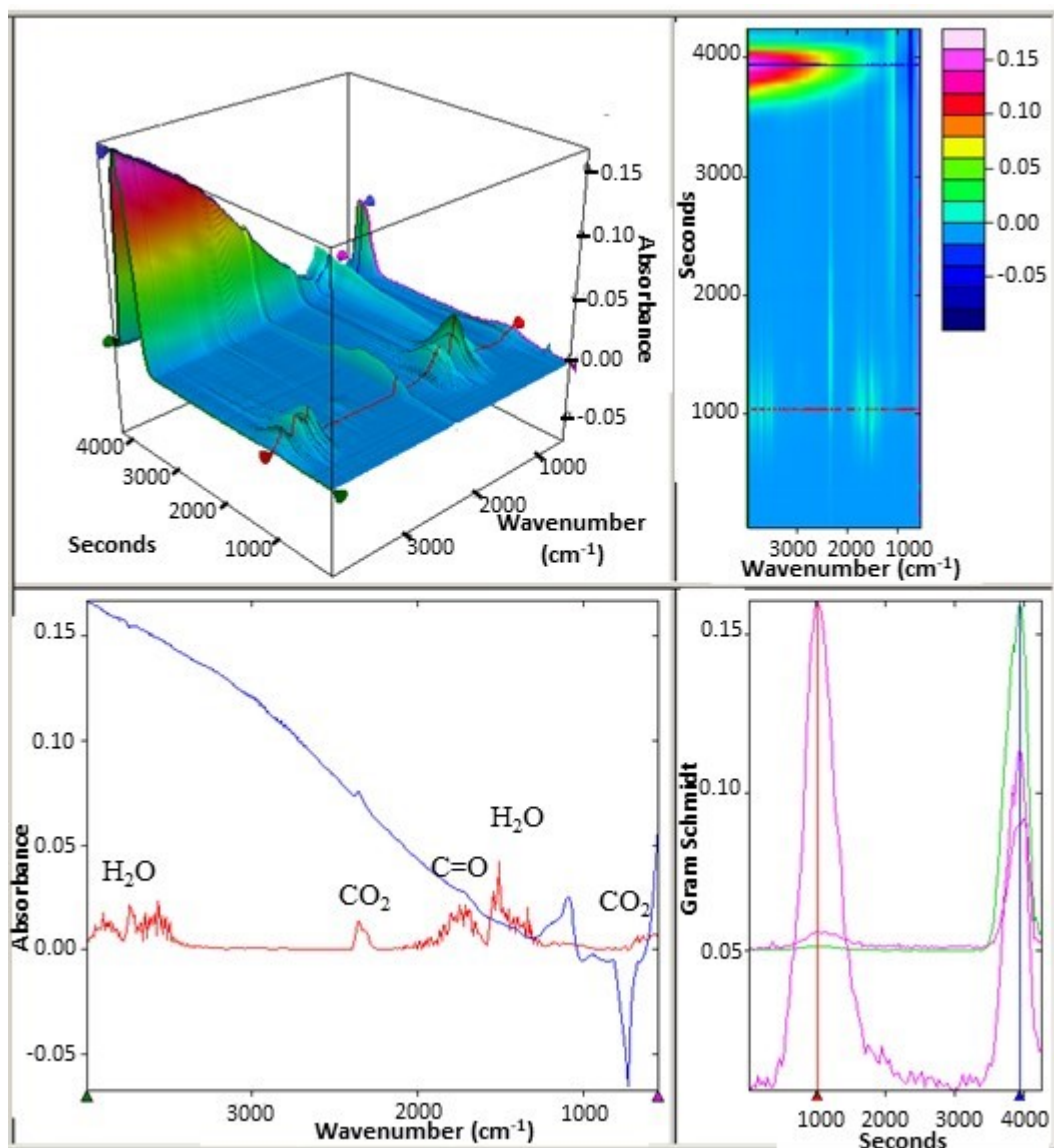


**Figure S9** TGA-IR analysis of ZAC1:5 during pyrolysis (top-left image: 3D plot of TGA-IR time-series, top-right image: color indication of IR spectra intensity, bottom-left image: IR spectra at 195 °C (red) and 700 °C (blue), bottom-right image: Gram-Schmidt graph).

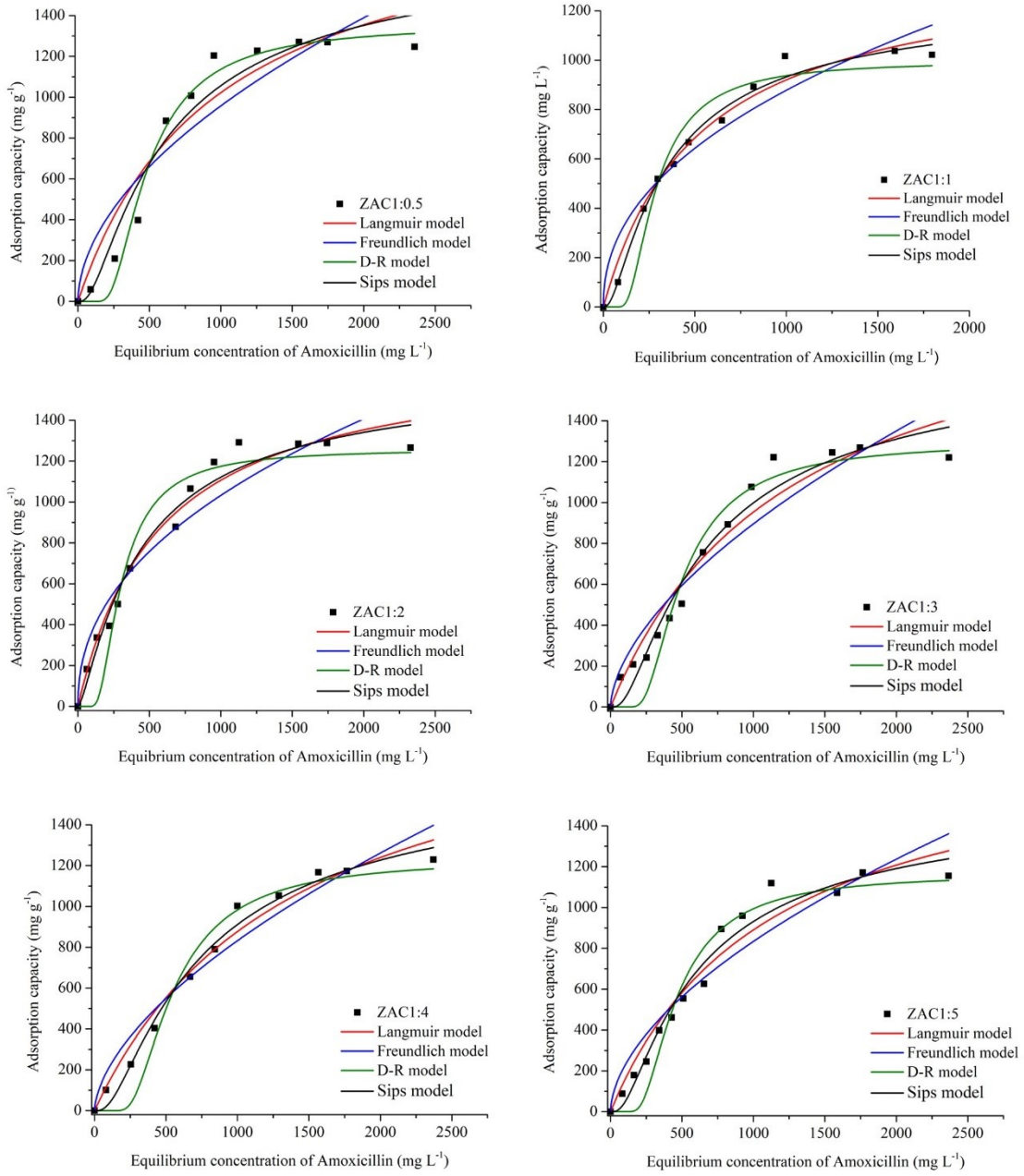


**Figure S10** Adsorption isotherms.

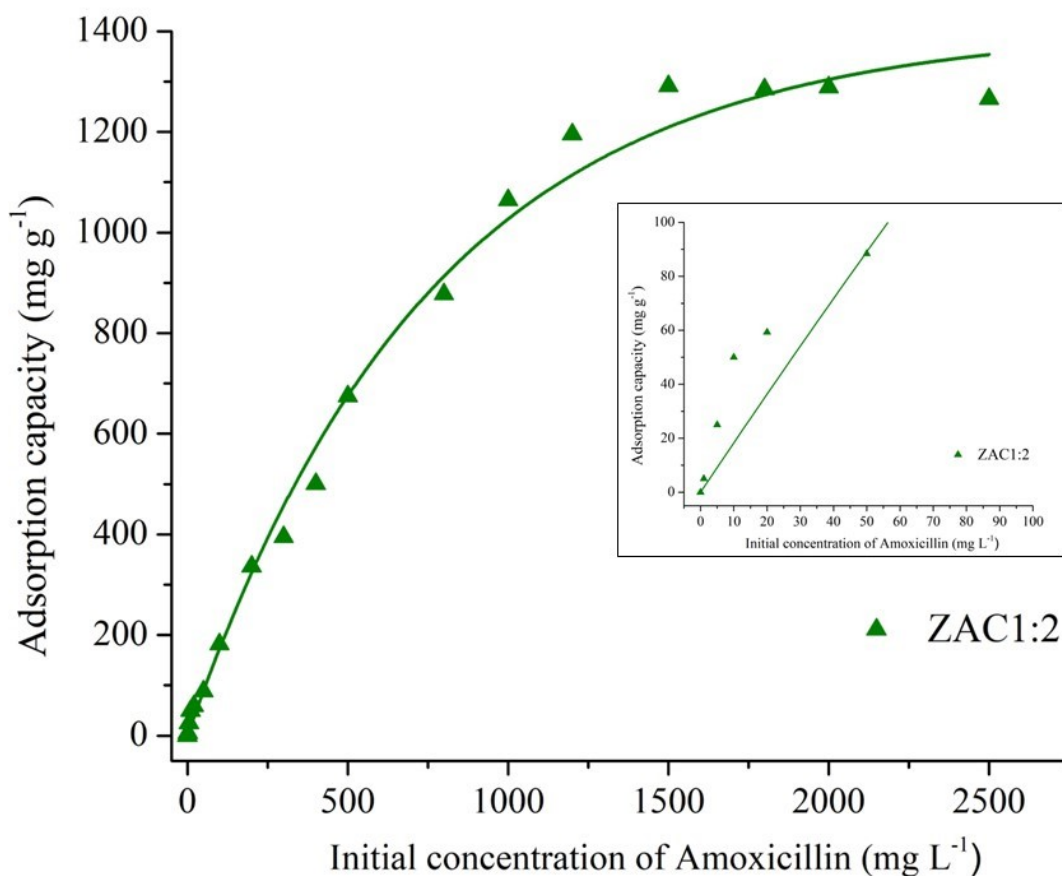


**Figure S11** Adsorption capacity dependence on the initial concentration of AMX using ZAC1:2.

High concentrations of AMX were utilized for adsorption to determine the maximum adsorption capacity of the activated carbons. However, 100% removal of AMX was obtained at low concentration (1, 5, 10 mg L<sup>-1</sup>) indicating the excellent performance of ZAC1:2 as an adsorbent even at such a low concentration of AMX (Figure S11). In addition, high concentrations of AMX would be applicable for treatment of aqueous or urine samples collected at source in places such as hospitals.

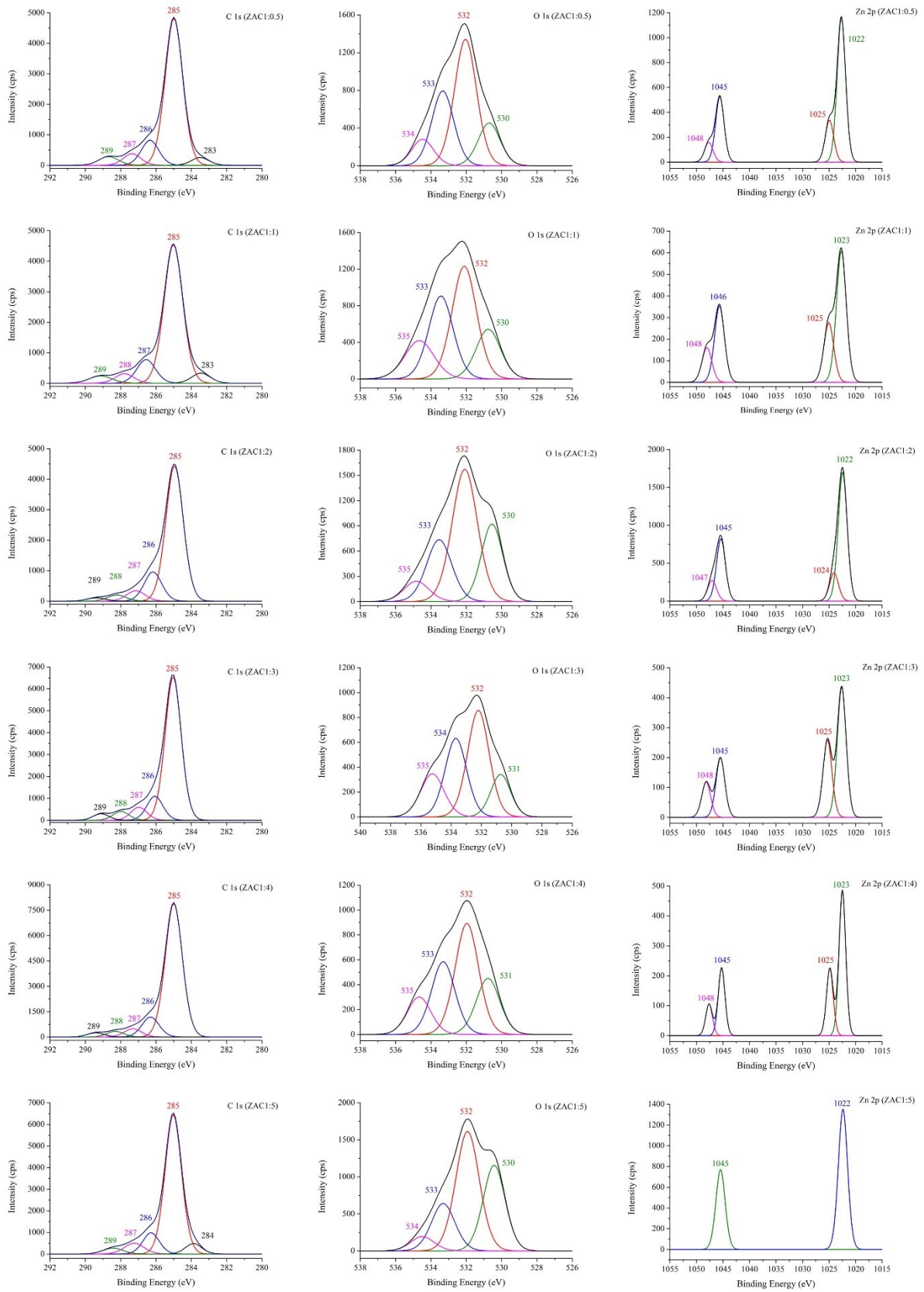


**Figure S12** XPS spectra of the activated carbon.

A replicate samples of ZAC1:2 was prepared and analyzed. After testing the porosity properties, the nitrogen adsorption desorption isotherm and the pore size distribution of both samples are shown in the figure S13. The results demonstrated that both samples have similar isotherms and pore size distribution curves, indicating the reproducibility of the nitrogen adsorption desorption isotherm and the pore size distribution of ZAC1:2.

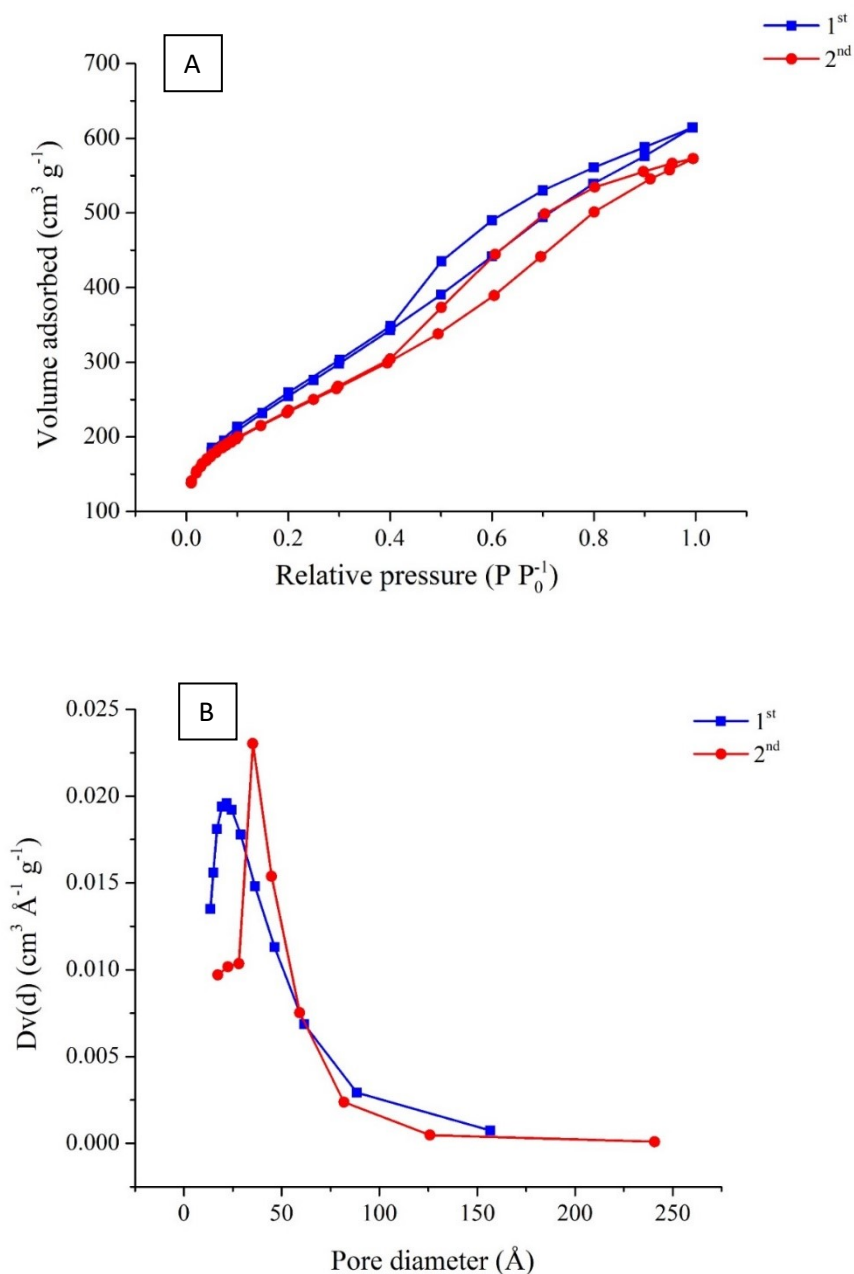


**Figure S13** A) N<sub>2</sub> adsorption/desorption isotherms of replicate samples of ZAC1:2 carbons and B) BJH pore size distribution of replicate samples of ZAC1:2 carbons.